



PCD coating polishing effect on the tool wear in high-speed milling of graphite

Rodrigo P. Zeilmann¹ · Cassiano Zanella¹

Received: 2 December 2019 / Accepted: 2 June 2020 / Published online: 12 June 2020
© Springer-Verlag London Ltd., part of Springer Nature 2020

Abstract

The manufacture of molds with increasingly shorter deadlines and costs requires tool manufacturers to improve their manufacturing processes. One of the ways is improving their electrode machining, because this process will affect directly in the result of the dimensional precision and production time of the mold. The usage of graphite as raw material for electrodes is known to be highly satisfactory since the graphite has the advantage of machining faster and allowing a great variety of geometrical forms; however, its main disadvantage is that the graphite also has a high level of wearing during the machining process. The cutting-edge preparations are used in order to reduce the effects of this problem, increasing the durability of the tools. In that interest, this paper has researched the effect of edge preparations, through the polishing of the PCD coating, on the wear of tools, in milling of graphite electrodes. Therefore, experimental tests were performed with untreated and polished tools, with abrasive brushes, and by drag finishing. The tests consisted in machining electrodes with analysis of tool wear, roughness, and characterization of the tools. The findings indicate that the edge preparation results in modifications on the coating surface, reducing the roughness value by a mean of 23%, and in the case of drag finishing process, a variation of the values reduction, since this process is more reliable and reproducible. With regard to the tools' wear, gains such as reduction of flank wear and a cutting length increase of up to 63% were noticed, in comparison with the original tools.

Keywords Machining · Polishing · HSM · Milling · Tool wear · Graphite

1 Introduction

The main processes used to manufacture a mold are milling and electrical discharge machining (EDM). By EDM process, the electrode's machining is one of the most critical phase due to the need for dimensional accuracy, surface quality requirements, and the amount of time spent in its production. This high exigency exists because the electrode is the tool used by EDM. Overall, the majority of electrodes is made of copper or graphite. The graphite is gradually taking up space in the tooling industry since it is considered faster and easier to manipulate for machining and it also has higher material removal rates by EDM process when compared with copper.

According to several authors [1–5], when milling graphite, the cut happens by a rupture process on the structure instead of plastic deformation; this happens due to its polycrystalline structure. The cutting region crushes the graphite right at the face of the tool cutting edge, while the tool is moving through the material. This process forms small particles that result in a graphite powder, rather than chips, like the type that occurs in the machining of metals.

For Klocke [1], Almeida et al. [6], Cabral et al. [2], and Schroeter et al. [7], the dominant wear mechanism on the graphite machining is the abrasion, which occurs due to the friction of the ultrafine powder flow; this can also be verified by a comb-shaped wearing. This type of wear occurs both in the tool's primary flank as in its flank face.

Carbide tools with polycrystalline diamond (PCD) coating are commonly used to increase the performance of cutting tools, due to its great hardness (80–100 GPa), low friction coefficients (0.04–0.1), and low adhesion [8, 9]. These characteristics make tools more expensive, compared with the standard tools used in the machining of common steels.

✉ Rodrigo P. Zeilmann
rpzeilma@ucs.br

¹ Area of Exact Sciences and Technology, University of Caxias do Sul, Francisco Getúlio Vargas Street, 1130, Caxias do Sul 95070-560, Brazil

Table 1 BC-15 graphite physical properties

Properties	Parameters
Density (g/cm^3)	1.85
Average grain size (μm)	7
Hardness (shore)	66
Electrical resistivity ($\mu\text{ohm.m}$)	12.5
Tensile strength (MPa)	66

Tokai Carbon [21]

The improvement of these tools, with the purpose to increase their life and reduce the quantity of setups in the machines, is one of the solutions found in the companies. As an example of the importance of these improvements, according to Zeilmann et al. [10] and Bhattacharyya et al. [11], failure of tools, as wear and break, represents about 20% of the downtime of a machine tool.

Although PCD coating has prominent properties, it has non-uniform grain sizes, random orientation of crystals, and high surface roughness which can be improved through the cutting-edge preparations [12–14]. Some studies, such as Bouzakis et al. [15] and Denkena and Breidenstein [16], show that these treatments help to achieve a better cutting performance due to improved cutting stability and reduction of cracks in the cutting tool edge.

The cutting-edge preparations most applied in finishing tools are polishing with abrasive brushes and the polishing method with drag finishing, since these are treatments that obtain an enhancement in the coating and have a simpler

application [17]. The polishing with abrasive brushes is used in applications that demand specific requirements for edging and surface finishing. During the polishing process, new abrasive grains of nylon filaments are constantly exposed as the wear progresses. This provides a consistent polishing action over the brushes lifetime [17, 18].

The drag finishing process has the characteristic of immersing the tool in an abrasive media. This media contains ceramic elements with known granulometries, used according to the polishing required [19]. The material removed is the result of relative movement between the tool and the abrasive media, which occurs due to the impact and contact of abrasive grains on the tool surface [20].

Considering the information shown before, regarding the cutting-edge preparations and the limited literature for the improvement of graphite machining, this study has the objective to evaluate the influence of the cutting-edge preparation, through the polishing of the PCD coating, using abrasive brushes and drag finishing. Furthermore, the use of cutting-edge preparation after deposition of PCD coating with high-speed cutting in graphite machining is the main contribution of this paper.

2 Material and methods

In this study, BC-15 graphite blocks from Tokai Carbon were used for the machining tests. The main physical properties of this material are shown in Table 1.

The tools used in the experiments were carbide tools of 8-mm diameter with total length of 100 mm, two edge, and PCD

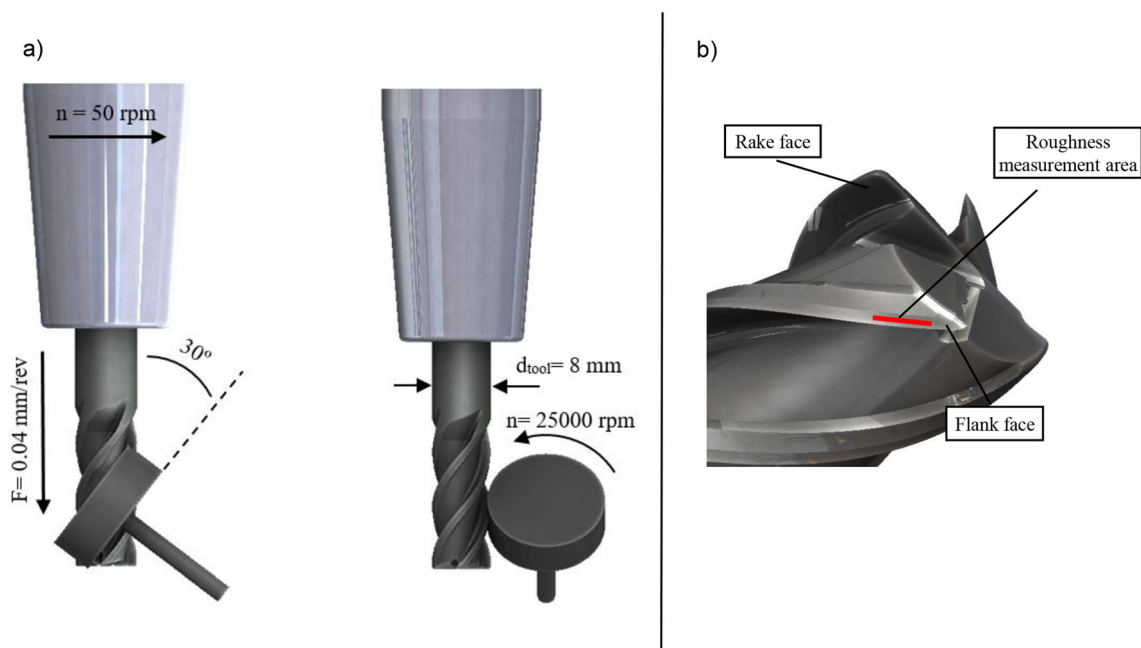


Fig. 1 Details from the (a) abrasive brushes polishing method and (b) locations of tool roughness checks

Table 2 Planning sequence and order of the experimental tests

Planning sequence	Polishing process	Order of tests (random)
1	PAB	4
2	PAB	2
3	PAB	9
4	FD	8
5	FD	3
6	FD	6
7	OS	1
8	OS	5
9	OS	7

coatings. All tools had a helix angle of 30° , the exit and incidence angle of 10° , a corner radius of 0.5 mm, and edge radius of $20\ \mu\text{m}$. The fixation of the tools happened through a Shrink Fit Chuck, of Haimer brand, of a HSK-E40 fixation model, with a g2.5 balancing, which assures a maximum run-out of $3\ \mu\text{m}$.

The tests were carried out on a Rödgers CNC machine, RXP 801 model with the maximum spindle speed of 42,000 rpm, 15 kW, and a maximum advancement of 60,000 mm/min.

To carry out the analysis and measurement of the flank wear on the tests, the optical measurement system and the Duo Video Swift from the brand Vision Engineering were used, these systems have a colored CCD video camera with 640×480 pixels resolution, $1\ \mu\text{m}$ encoder resolution, and a $\times 100$ maximum zoom.

The roughness measurements were performed with the portable surface roughness tester, SurfTest SJ-201P Mitutoyo model, which has a measurement capability of Rz of 0.02 to $350\ \mu\text{m}$ with a diamond tip and measuring force of 4 mN.

The polishing with abrasive brushes was carried out at the university, in the same polishing conditions as OST [22]. The sponge was fixed in a mini pneumatic manual grinding with a speed of 25,000 rpm. This mini grinding was fixed on the table in a machining center. Figure 1 illustrates how the polishing procedure occurred. The tool was assembled in a clamp in the machining center at a speed of 50 rpm in the direction opposite to the tool cut and feed (f) of 0.04 mm. The sponge was at an angle of 30° , because this is the tool helix angle. The process time was 5 min.

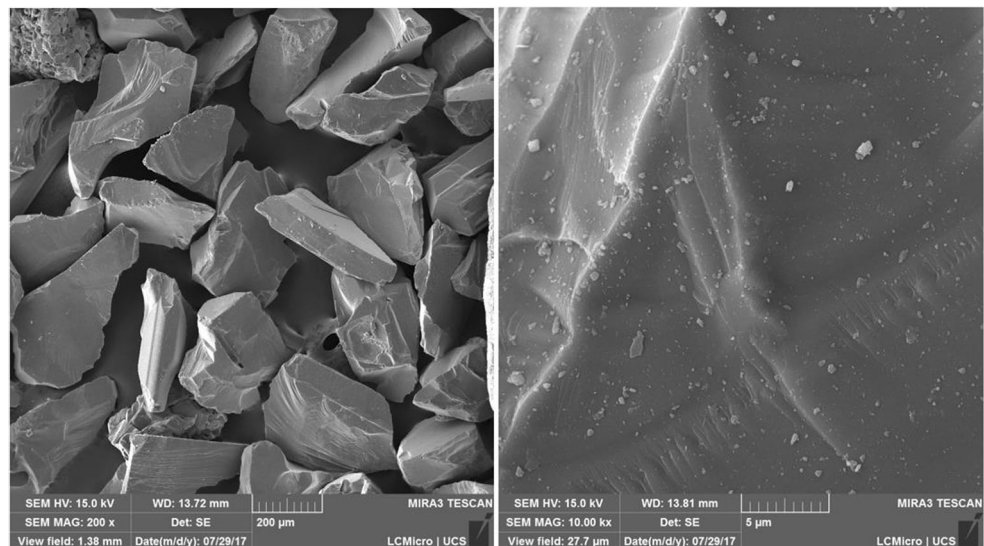
The drag finishing process was performed at Lesi Tools Company, with an abrasive media HSC 1/300, indicated to obtain high surface quality, approximately 0.5 Rz, and for polishing process in coated tools [23]. The abrasive media and the drag machine used in the polishing process are from Otec. The media used consist of a mixture of 30% silicon carbide (SiC), with a grain diameter of $200\ \mu\text{m}$, and 70% of walnut shells with diameters between 0.8 and 1.3 mm [23]. The rotations of the tool and machine tree were 40 rpm. The tools remained rotating on the abrasive media in the cutting direction for 10 min.

The media characterization occurred in the scanning electron microscope (SEM), where the grains of the abrasive material were fixed to a base and covered with a gold layer, due to technical aspects of the SEM analysis. The magnifications used were $\times 200$ and $\times 10,000$. An analysis by energy disperse X-ray detector (EDS) was also performed with the objective of identifying the substances that constitute the material.

The characterization of the abrasive brushes was performed in the SEM with $\times 150$ and $\times 5,000$ magnification, in order to verify the surface and the disposition of the brushes and the abrasive material. The EDS analysis was also performed.

New samples were used for the media analysis and for the abrasive brushes, without being used for another purpose, in order to have no modification in the structures and no contamination with other materials.

Fig. 2 SEM of the silicon carbide (SiC) grain from the drag finishing media



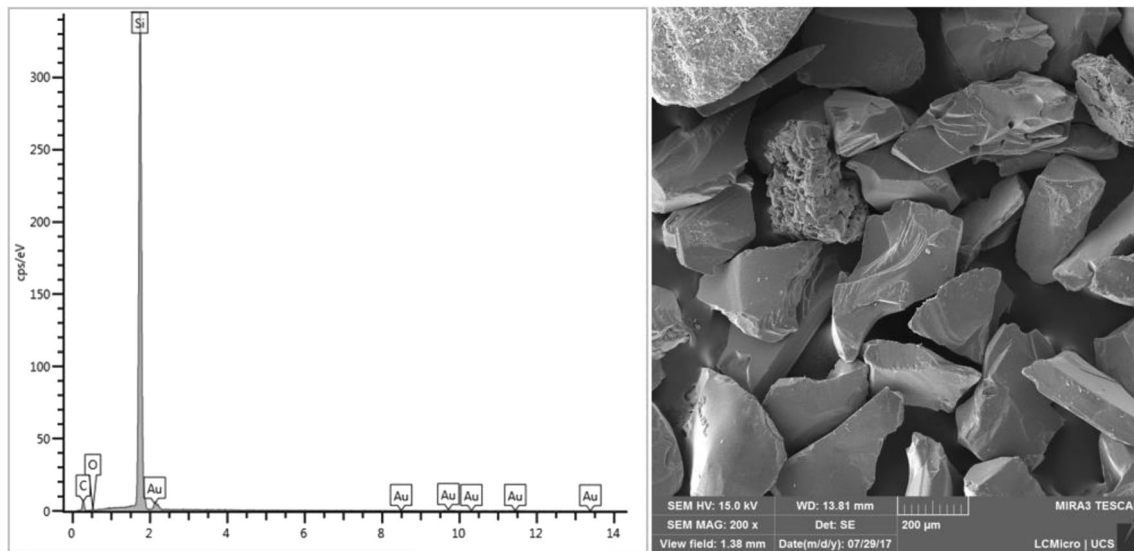


Fig. 3 Media EDS analysis

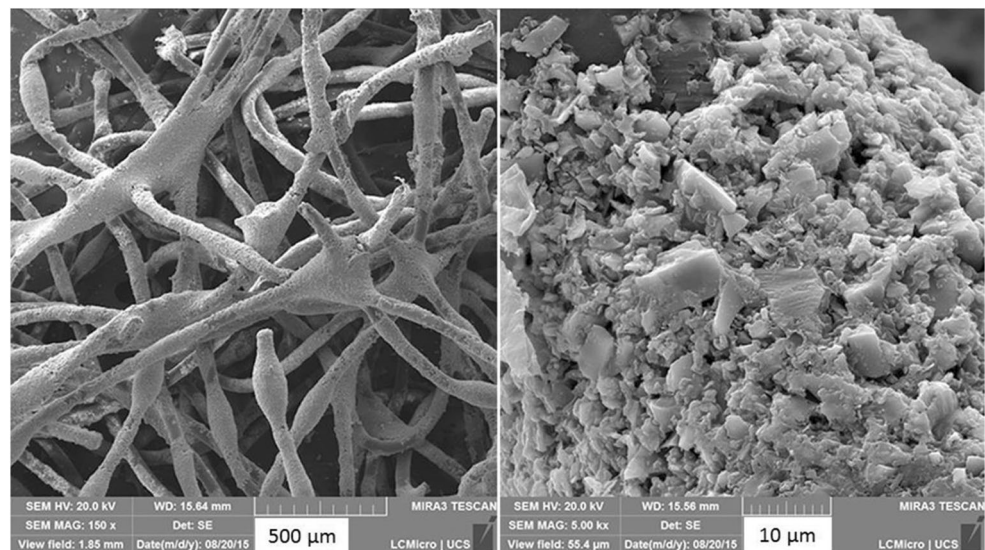
The characterization of the tools was carried out using the digital microscope, with magnification of $\times 150$, and by SEM, with magnifications of $\times 250$ and $\times 2,500$. The tools were positioned in the SEM through a fixation device with position adjustment for the view of the edge, face, and flank. Measurements of diameter, helix angle, and edge radius were performed using the Vision Engineering Swift Duo optical and video measurement system, which has a colored CCD video camera with 640×480 pixel resolution, $1 \mu\text{m}$ encoder resolution, and a $\times 100$ maximum zoom.

In order to evaluate the treatment effects on the tool surface, roughness measurements were performed in the flank region, close to the main cutting edge, according to Fig. 1 b. The cutoff (λ_c), chosen for the measurements, was 0.25 mm , because, even though the roughness values R_a are higher than the normal working range, the total measurement length

makes the measurement with an impossible upper cutoff, since the tool's propeller profile is curvilinear and superior to the maximum curvature allowed by the roughness tester. For the measurements, three reproductions were used for each analyzed region, two regions per tool, representing six values of roughness, a total of 18 measurements for each tool treatment.

With the objective to characterize the graphite and qualitatively analyze the surface of the graphite, images were taken by SEM on two surfaces of a graphite workpiece. The graphite block was fractured in half so that it was possible to check the surface without the influence of the milling. Another surface was machined, so that it was possible to verify the changes in the material basal planes due to the machining. This characterization aims to aid in the understanding of the high abrasive power of the material because of the differences of resistance

Fig. 4 Detailed view of the polishing brush (adapted from 17)



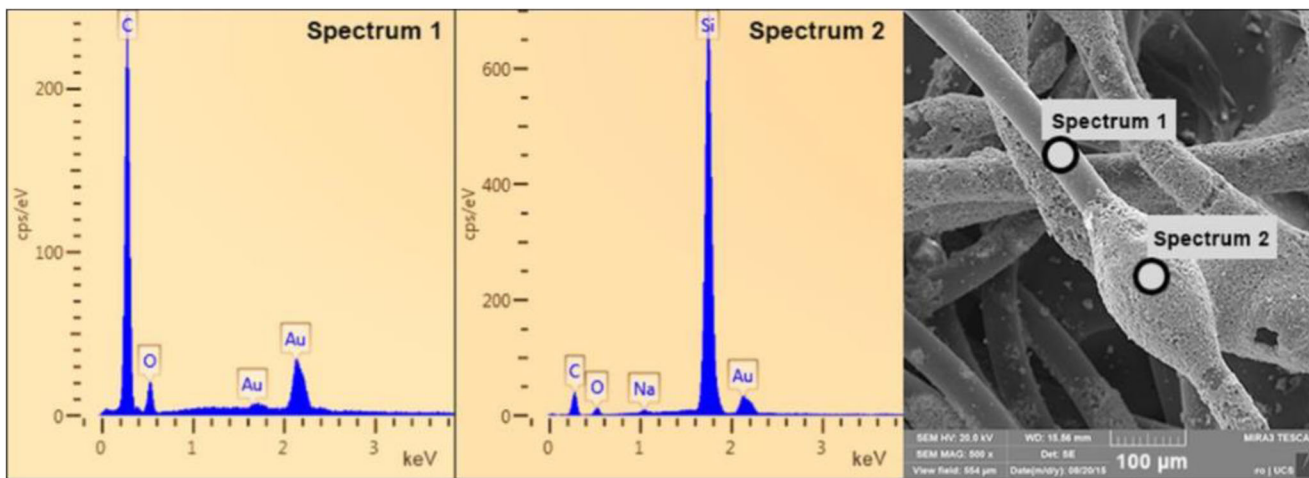


Fig. 5 Brush EDS analysis (adapted from 17)

in the structural bonds of the graphite. Due to this purpose, machined surface analysis was performed only with the original milling cutter.

All tests were carried out on a real production of electrodes, because experimental time was long. The tests only occurred during the rough steps of the electrodes, as a result of the greater ease of standardizing the cutting parameters and the possibility of removing more material. The parameters were defined according to the technical catalog of the manufacturer and the execution of a previous test considering high parameter levels, verifying the tool wear, the behavior of the machine, and the graphite block.

In order to understand the tools' wear presented and to reduce the number of variables influencing the machining process, some parameters were kept constant. The machining strategy used was concordant with a cutting speed (v_c) of 700 m/min, feed rate (f_z) of 0.2 mm, axial depth (a_p) of 0.7 mm, and lateral depth (a_e) of 4 mm.

For the execution of this work, two edge preparation processes were used: the polishing with abrasive brushes (PAB) and the finishing by drag media (FD). For the tests, the tools were also used in their original state (OS), in order to verify the influence of the edged treatments on their life cycle. In order to increase the reliability of the results, for each test, two replicates were performed, totaling 9 tests. Table 2 shows the planning sequence and order of the tests. The order in which the tests were performed was random for better statistical reliability.

As an output variable of the test, tool wear was verified by measuring maximum flank wear (VB_{max}) at every 200 m of machining. This machined length measurement occurred through the machining center software which reports the machined length per tool. The tests were conducted until one of the end-of-life conditions had been reached; the conditions for this end-of-life were of a maximum flank wear of 0.2 mm or the chipping of the tool.

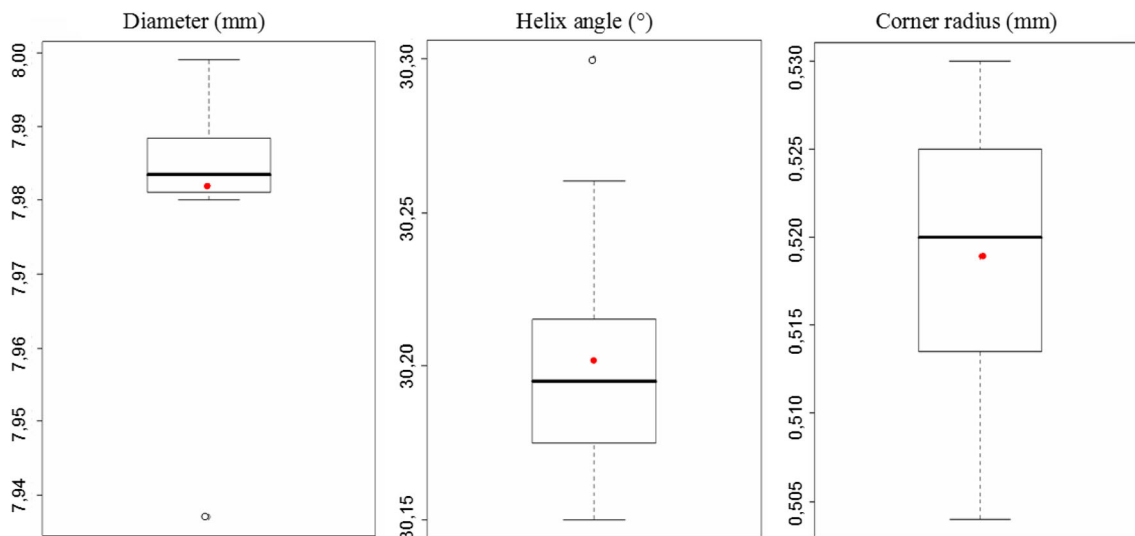


Fig. 6 Dimensions of diameter, helix angle and corner radius of the tools

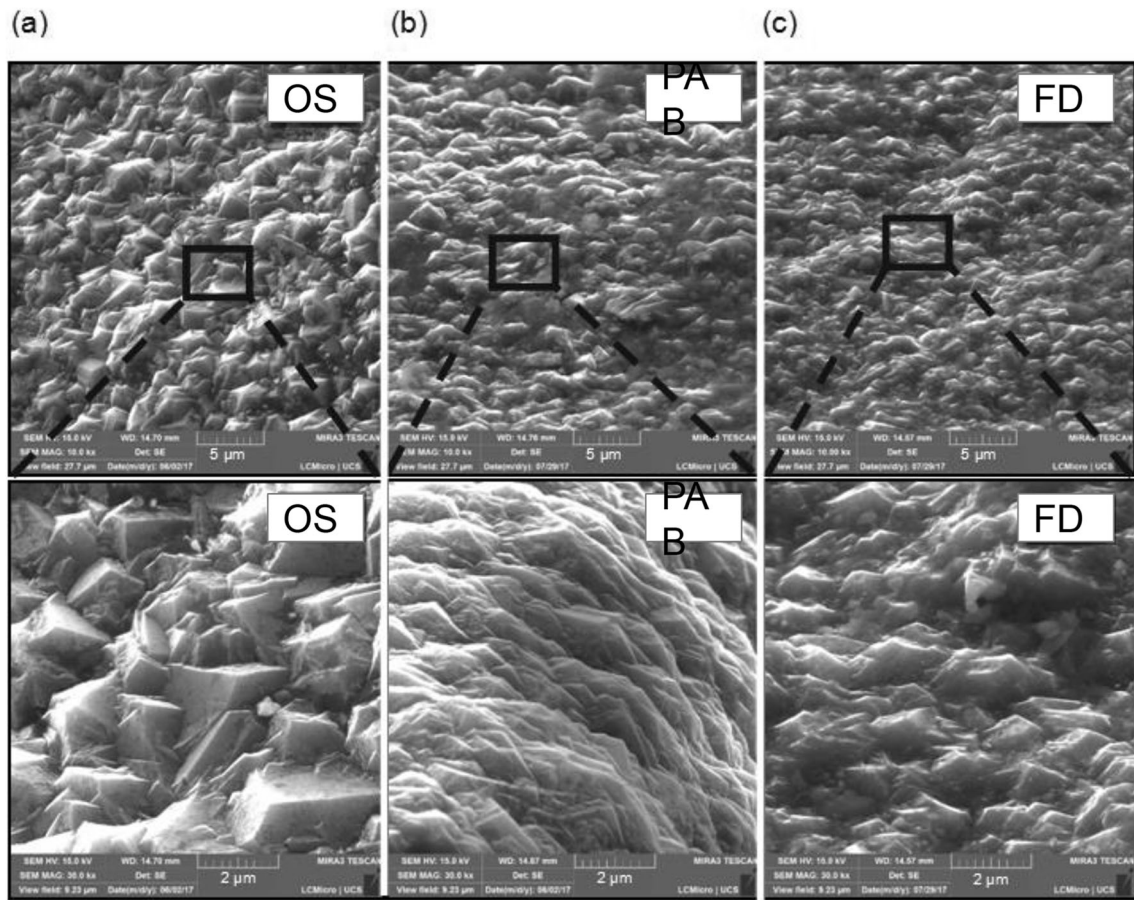


Fig. 7 SEM analysis of tool surfaces with different treatments: (a) original state - OS; (b) polishing with abrasive brushes - PAB; and (c) finishing by drag media - FD

The Fischer’s test was applied with the purpose of comparing the pairs of means and verifying if there was or if there was not a difference in the values obtained. A

significance level of “ α ” of 1% was used. The definition of the sequence for the tests was made to avoid the influence of other factors that could not be controlled.

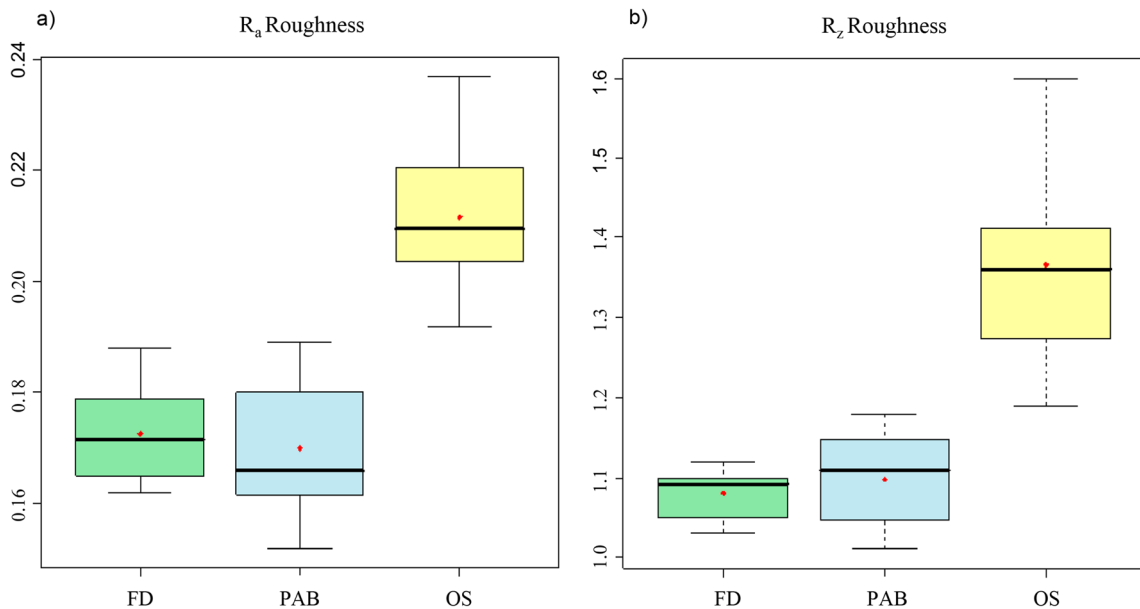


Fig. 8 Tools roughness values: (a) Ra roughness; and (b) Rz roughness

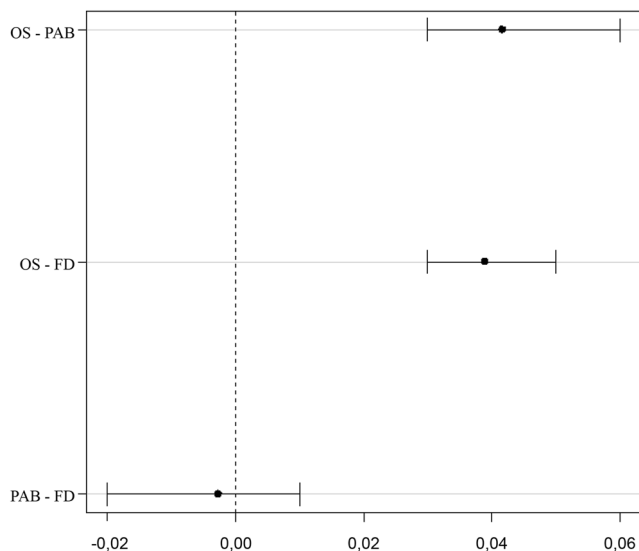


Fig. 9 Fischer analysis of roughness values

3 Results and discussion

3.1 Drag finishing media characterization

The media analyzed, known commercially as HSC 1/300 (from OTEC GmbH.), consist of walnut shell grains of homogeneous size and silicon carbide grains (SiC). The majority of the silicon carbide grains has acute angles with average size of 300 μm, which, according to Tikal [24], are recommended for improvement of the finishing and removal of droplets. Figure 2 shows the image of the profiles of the silicon carbide grain (a) and a detail view of the silicon carbide grain (b).

In order to confirm the material of the abrasive media, an X-ray energy spectrometry dispersive (EDS) analysis was performed (Fig. 3).

According to EDS analysis, the main chemical element presented in the media, without regard to the walnut shell grains, is silicon, which corroborates with the media manufacturer’s information that the material is silicon carbide.

3.2 Abrasive brushes characterization

With the characterization of the abrasive brushes material through the SEM, according to Fig. 4, it is possible to observe the geometry, construction, and shape of the abrasive material. On the left image of Fig. 4, it is possible to identify in a more macro way the structure of the sponge (a), which consists of a wire mesh of approximately 50-μm diameter with an abrasive material adhered. On the image to the right (b), it is possible to observe in a more focused way the crystals of the abrasive material, which present themselves in varying dimensions, going from approximately 1 to 10 μm, with a fragmented appearance.

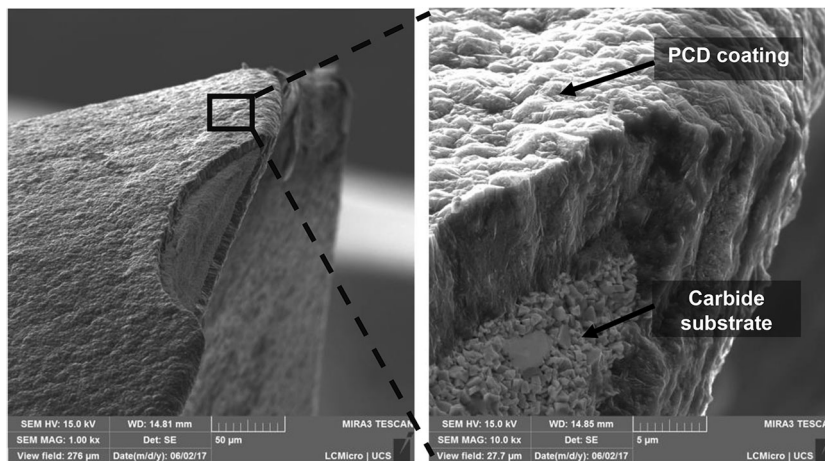
An analysis by EDS was carried out in order to define which materials compose the brush, according to Fig. 5. By technical aspects of the analysis, the materials were covered by gold.

The first analysis of the spectrum 1 region was performed at the place where the fiber is exposed. In this position, the analysis supports that the fiber is basically carbon, which validates the sponge manufacturer’s claim to be nylon. The second analysis performed in the spectrum 2 region was made where the abrasive material was deposited. The result indicates a high concentration of silicon, which may probably characterize a silicon carbide material. Both characterizations demonstrate the use of silicon as an abrasive material in the processes of drag finish and abrasive brushes, being that its differential is the form of the polishing process application.

3.3 Tools characterization

With the purpose to map and validate the tools for the tests, removing possible defects, the tools were characterized in two ways. The first one was the macrogeometric form, measuring the dimensions of diameter, helix angle, and corner radius of the tools, and the second one was the superficial form, through the roughness and the images obtained by SEM. The

Fig. 10 Coating condition and thickness



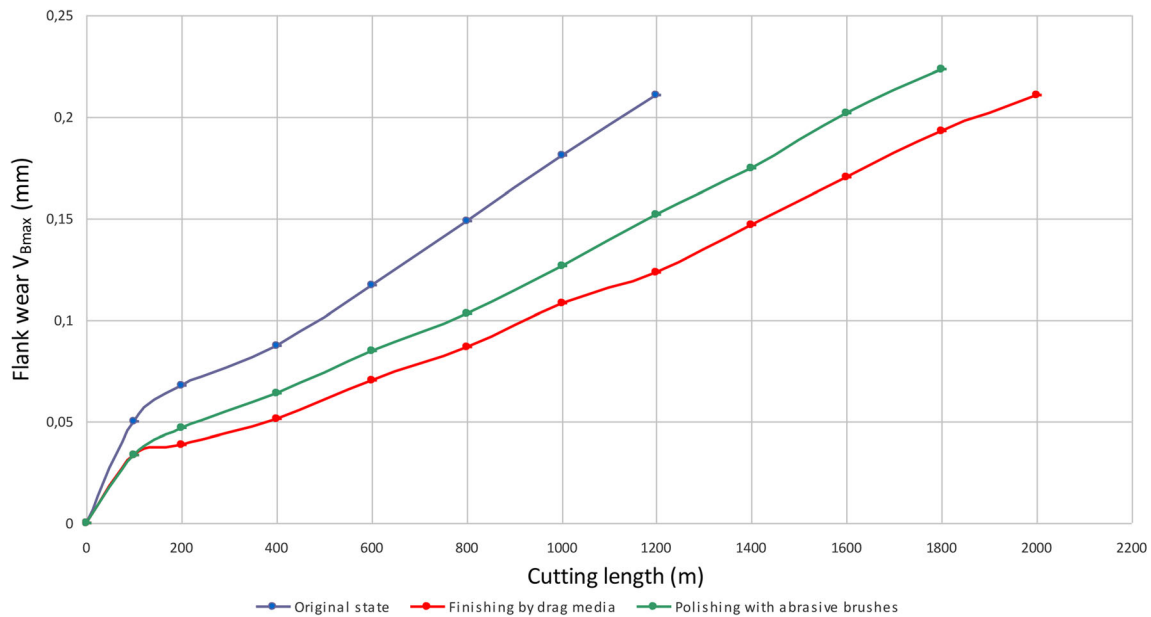


Fig. 11 Tools' wear behavior curves

geometric macrocharacterization, as visualized in the boxplot graphs, Fig. 6, brings the data to a sample of the tools.

These data indicate that the tools have similar dimensions, the average diameter being around 7.98 mm, the helix angle around 30.20° , and the corner radius in 0.52 mm. Two tools had outlier values, one with respect to the diameter, which was 7.94 mm, and another with respect to the helix angle; this one presented the value of 30.30° . These two tools were discarded and were not used in the experiments, since this variation may be due to a manufacturing defect and could alter the testes results.

With respect to the tool surface characterization, Fig. 7 shows a view of the tools' edge surface with the three processes: original state (OS), polishing with abrasive brushes (PAB), and finishing by drag media (FD). Looking at the images of Fig. 7, it is possible to distinguish the results from the different cutting-edge treatments: original state (a), abrasive brushes (b), and drag finishing (c). The original tool (OS) presents the PCD crystals with an apparent larger width with an average of around $2 \mu\text{m}$.

In the image of the original tool, it is also evident that the PCD crystals have a growth orientation perpendicular to the surface of the tool. The topography in the original tool resembles the analyses performed by Ralchenko et al. [12] because the diamond grains have well-defined faces and edges with more acute corners. This characteristic, according to Klocke and König [1], means that the resistance to abrasive stresses in the machining process is not so high when compared with rounded edges.

Looking at Fig. 7, the tool that has undergone the polishing process with abrasive brushes (PAB) presents a reduction when compared with the original in the measurements of width of the crystals, less than $1 \mu\text{m}$. Also evident is the reduction in crystal heights compared with the original tool and loss of clear definition of the edges.

According to Gunnars and Alahelisten [25] and Murakawa et al. [22], this happens because of the relatively high level of compressive residual stresses in diamond coatings, usually caused due to their lower coefficient of thermal expansion than substrate, being a sintered tungsten carbide alloy, and

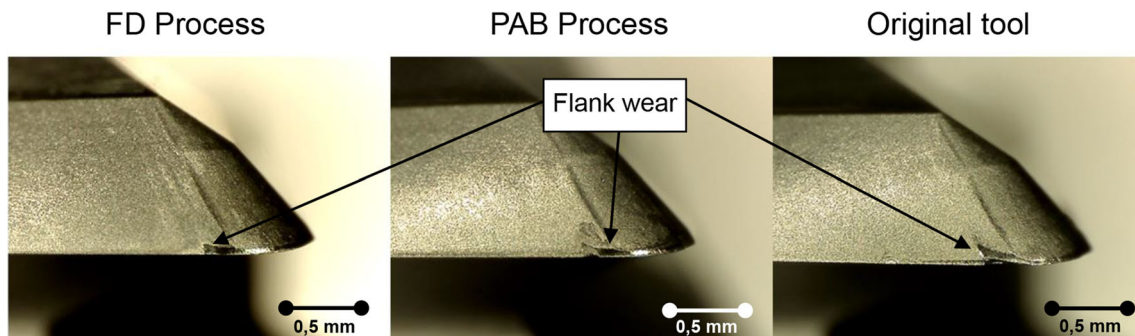
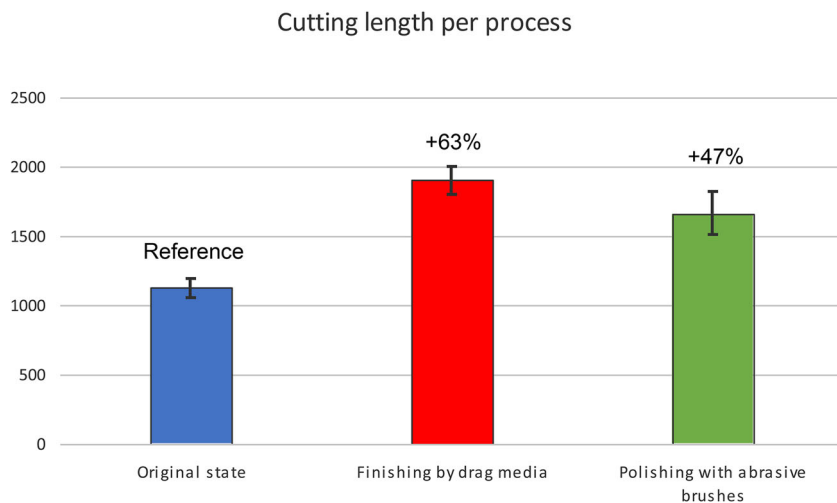


Fig. 12 Tool wear

Fig. 13 Cutting length (tool life)



which are responsible for the cracks and breaks of PCD crystals.

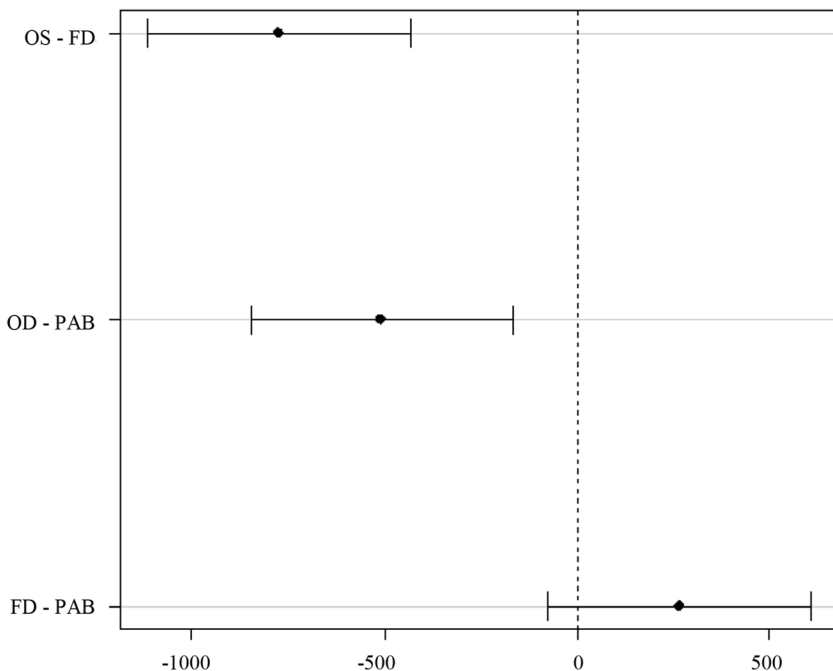
Following the tendency of the tool with abrasive brushes polishing, the tool in which the drag finishing process (FD) was carried out showed a reduction in the crystals sizes. However, this showed a greater roundness of the edges of the crystals and a smaller definition of their peaks.

With the purpose to highlight the changes promoted by the cutting-edge treatment and the analysis done through the SEM, Fig. 8 presents the roughness values Ra (a), and Rz (b), for the tools with the finishing process by drag finish (FD), abrasive brushes (PAB), and original tool (OS), performed in the region of the flank near the main tool edge.

The boxplots of the Fig. 8 show that the original tool has the greatest variation and the highest values of roughness for both Ra and Rz roughness, which reinforce the analysis performed through the images of Fig. 7 above. The tools with the drag finish process, and abrasive brushes process presented statistically the same values of roughness.

The analysis performed through Fischer’s multiple comparison test (Fig. 9) corroborates the analysis performed by the boxplots of Fig. 8, in the first line is the comparison of the means of the OS tools with the PAB, and in the second line is the comparison of the means of the tools OS and FD; these indicate that they have significant differences, since they are not crossing the vertical line at zero.

Fig. 14 Fischer analysis of machined length



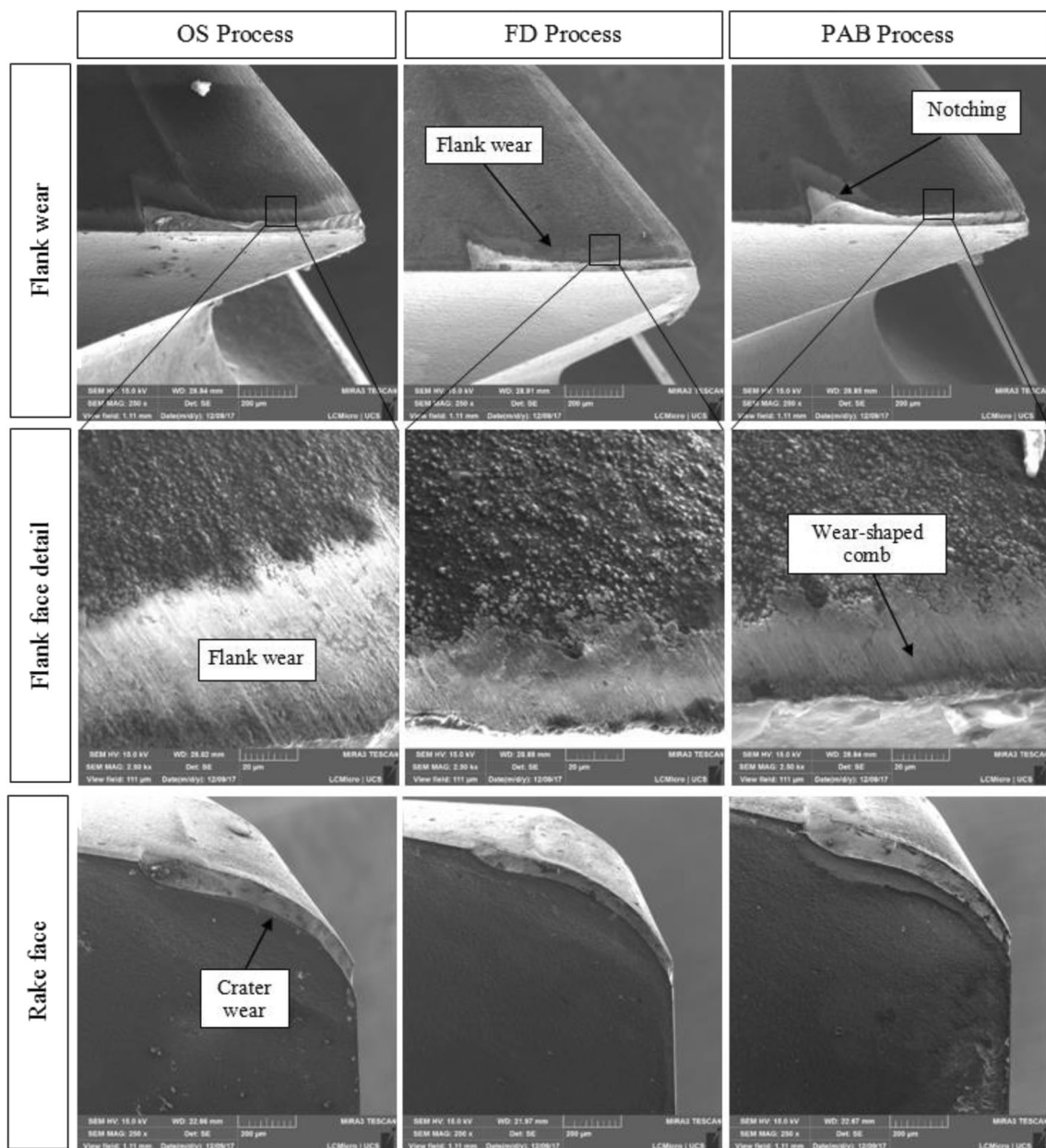


Fig. 15 Tool wear images

The comparison between PAB and FD tools crosses the vertical line, which indicates that they are statistically similar.

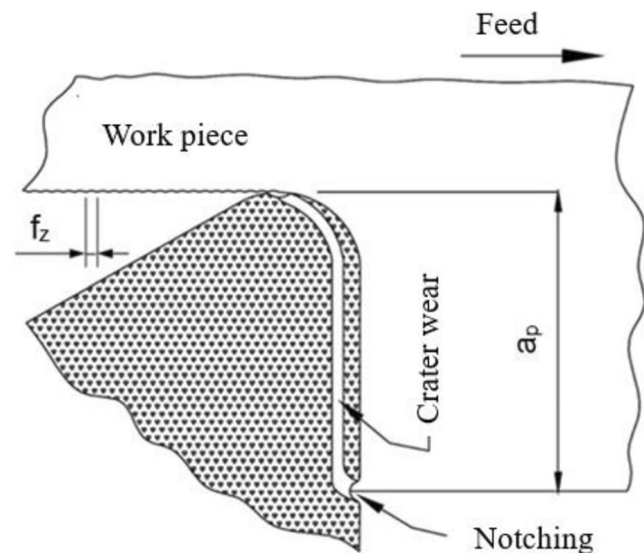
The difference that can be viewed through the graphs of Fig. 9 is that the drag finish generated a more homogeneous surface between the tools, since the variation between them was smaller when compared with the tools with the PAB process. According to Tikal [24], this lower variation can be explained because the drag finishing process has more control over the variables. The thickness and the condition of the coating layer were also verified through the SEM (Fig. 10).

In the microscope measurements, the mean thickness was $7.3 \mu\text{m}$, with a standard deviation of $0.37 \mu\text{m}$, which falls within the thickness range for the PCD coating.

3.4 Tool wear

The tools' wear behavior curves for the three cutting-edge treatments were generated (Fig. 11). The measurement points reflect the maximum flank wear (VB_{max}) measured in the tools every 200 m of machined length. Only the first two measurements were performed with a range of 100 m in length in order to better identify the first stage of the wear. The three curves identified in the graph were the result of a test and its two replicates; these led until the wear VB_{max} reached the value of 0.2 mm. As a characteristic of the three curves, the beginning is accentuated followed by a more stable growth near linearity.

Fig. 16 Schematic representation of crater and notching wear generated during machining [2]



According to Machado et al. [26], this accentuated beginning is known as stage one—adaptation, which is an adequacy to the tribological system involved. Following, stage two, stabilization, is the most stable cut phase. None of the curves entered stage three—catastrophic wear.

Through the analysis of this graph, it is possible to notice that the wear curves are almost constant. According to Klocke and König [1], this phenomenon is known as a flank uniform deterioration phenomenon. According to Zeilmann [27] and Li [28], this increasing wear behavior is typical.

Through the graph curves, it is possible to notice already in the first measurements that the original tools (OS) presented a maximum flank wear greater than the tools with treatment (FD and PAB). The graph also shows the very similar behavior between the curves of the tools with the process of finishing by drag and the process of polishing with abrasive brushes.

However, the tools with PAB treatment demonstrated a greater variation among the tests, when compared with the FD process, even though both presented higher performances than the tools with OS.

In order to illustrate the wear variation found in the tools shown in the previous chart, Fig. 12 shows the cutting-edge images of a sample each tested conditions at the machined length of 1000 m. It can be seen that, in the tools with FD and PAB processes, the flank wear behaved in a similar way, while in the original tool, wear was advanced. This variation in wear presented in the original state (OS), compared with the tools with the treatments, reinforces the improvement generated by the cutting edge, which is related to the reduction of the roughness in the coating. This improvement mitigates the contact of the graphite chip with the tool's surface, which may be related to the reduction of the wear. As Klocke and König [5] stated, this wear is called uniform deterioration flank phenomenon. And according to Zeilmann [15] and Li [16], this increasing wear behavior is typical.

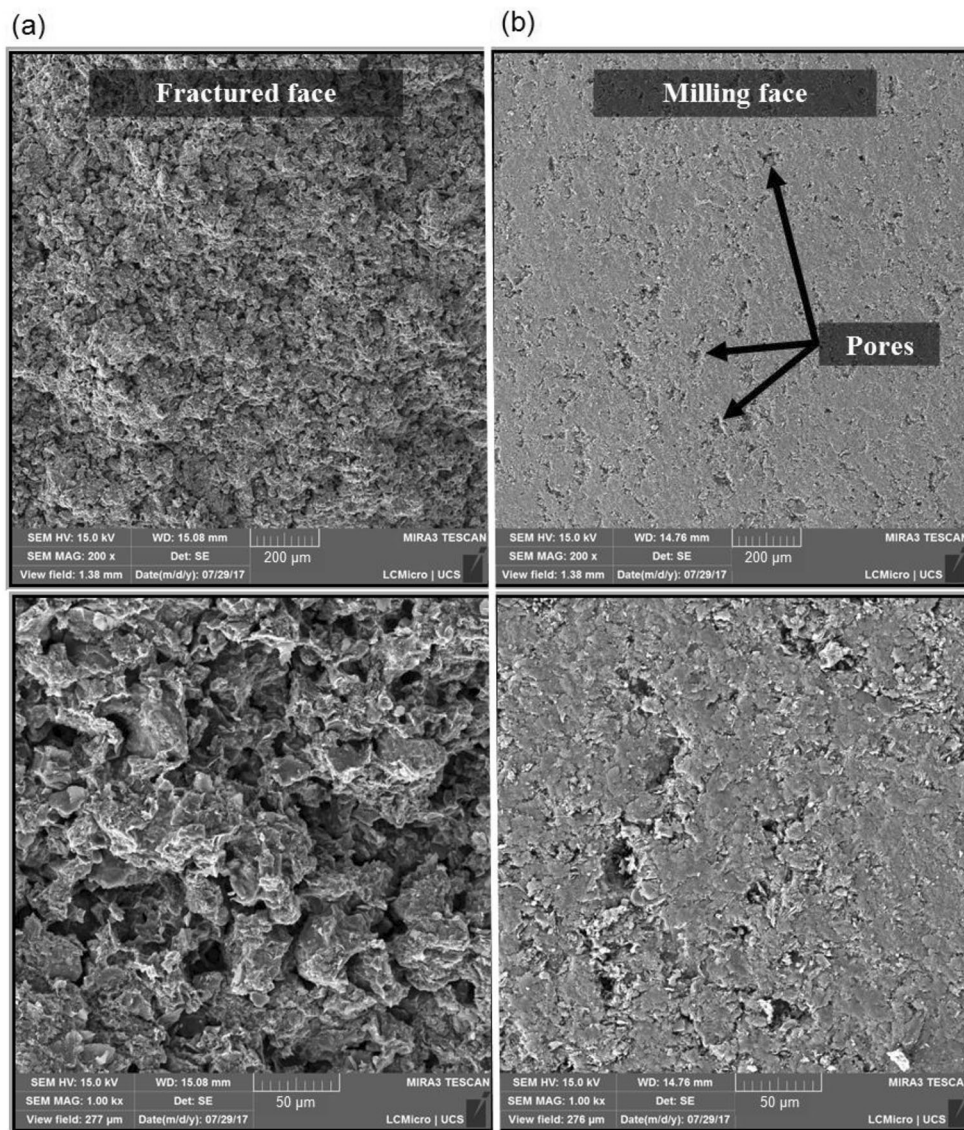
To compare the performance of each process, a graph with the average of cutting length performed by the tools is shown in Fig. 13 until they reach VBmax of 0.2 mm. Due to the impossibility of finishing the tests at the exact instant of wear at 0.2 mm, the cutting length values have suffered a linear interpolation to the value of 0.2 mm wear.

In the figure, the percentage gain of cut length is also identified using the original cutters as reference. The two cutting-edge processes presented considerable gains, the drag finishing with an average increase of 63% and the finishing with abrasive brushes of 47%. The analysis performed through Fischer's multiple comparison test (Fig. 14) corroborates the analysis performed by the graph of Fig. 13, where in the first line is the comparison of the means of the OS tools with the FD, and in the second line is the comparison of the means of the tools OS and PAB; these indicate that they have significant differences, since they are not crossing the vertical line at zero. The comparison between the FD and PAB tools crosses the vertical line, which indicates that they are statistically similar.

A possible link regarding the gain in the length machined by the treated tools, having as a reference the untreated tools, is the roughness values presented in the characterizations of the cutters. The roughness of the two treatments performed showed a reduction in comparison with the original tool, and the abrasive brushes polishing process also showed a greater variation in the measurements, compared with the drag finish.

As a comparison, in the experiment carried by Bouzakis et al. [29], the abrasive brushes polishing process on TiAlN coating carbide inserts used in milling Inconel 718 showed an increase in the tool life by 30% compared with the original tool without treatment. Zeilmann et al. [10] present in another experiment that the process of finishing by drag in high-speed steel tools presented a 50% reduction of VBmax in face milling of the AISI P20 material.

Fig. 17 (a) Fractured and (b) machined graphite surfaces



In order to detect dominant wear mechanisms in the process during the experiments, this section presents the images generated through SEM and the respective analyses of the tested tools. Analyses were done on all tools. SEM images were made on only one edge, for each condition (Fig. 15).

The wear presented was similar for all conditions tested. Apparently the most dominant wear mechanism was abrasion, which results in flank wear. This wear occurs commonly in graphite machining and is generated predominantly by the ultrafine powder flow of graphite, as observed by several researchers [1, 2, 6, 7, 30].

A characteristic wear in the graphite machining, also generated due to the abrasion mechanism, known as comb-shaped wear, appears subtly in this figure. This wear generates grooves in the tool due to the flow path and friction of the graphite powder [1].

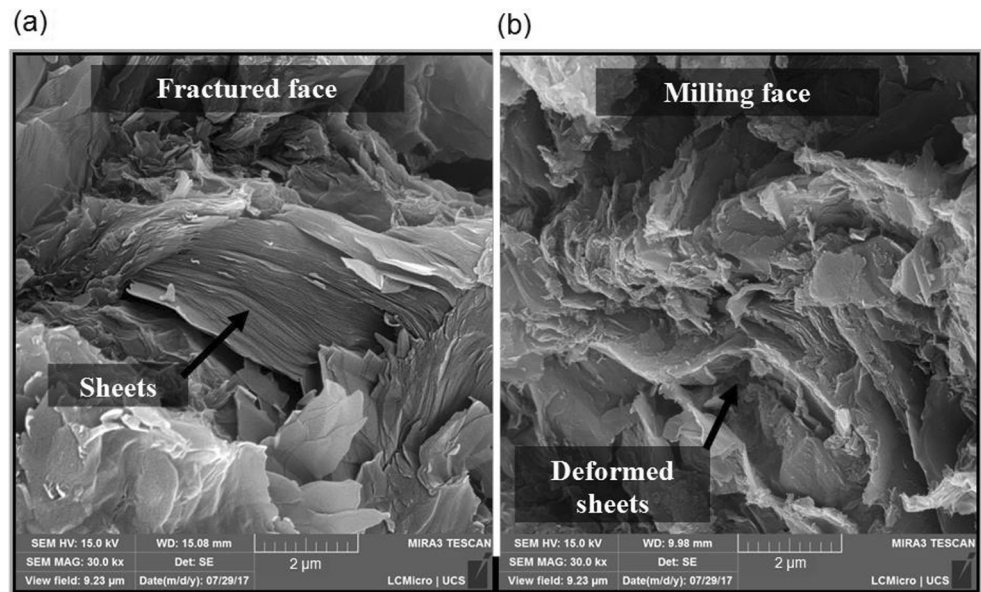
Finally, notching and crater wear are identified, where the latter consists of a concave section on the inclined face of the tool, formed by the action of graphite powder that comes into contact against the face of the tool during machining. This effect is shown in Fig. 16.

This process leads not only to the formation of a crater but also the generation of the notches, which function as exit paths for the flow of graphite dust from the cutting edges [2, 6, 29].

As can be seen in Fig. 15 and diagrammatically in Fig. 16, the three different processes generate the same wear mechanisms. This occurs because it is related to graphite machining and the graphite flow. In this case, the cutting-edge preparation can only reduce the wearing and improve the tool's life.

With the purpose to identify the reason why the graphite machining generated a high wear, the graphite characterization was conducted. The analysis was performed in a graphite block where

Fig. 18 Graphite structure: (a) fractured face ; and (b) milling face



one of the surfaces was machined with the same parameters as those used during the tests and with the original milling cutter (b), and the other surface was fractured through external impact (a), with the purpose to verify the structure and topography of the block without having undergone by milling process. Images of these surfaces can be seen in Fig. 17.

The two images on the left side of this figure refer to the fractured surfaces, the first with the magnification of $\times 200$ and the second with $\times 1000$. The two images on the right side refer to machined surfaces with the same magnifications. In the fractured surface image, it is possible to verify, in a qualitative way, the heterogeneity of the graphite grains and the roughness of the surface present in the structure of the graphite coming from the graphite block fabrication process, which is responsible for the porosity of the material.

According to Pierson [31] and Huo, Lin, and Dalgarno [32], these graphite characteristics are due to the material being polycrystalline and the orientation of the crystals being random. In the macroscale, the graphite used in EDM has thermal and mechanical isotropic performance, besides being fragile. Therefore, the imperfections of the sizes and shapes of crystal graphite, such as vacancies, stacking faults of graphite blades, and declination when the planes are not perfectly parallel, have a great influence on the properties and formation of graphite.

The porosity of the material is also visible in this condition, as identified in Fig. 17, in which the dark regions represent the porosity, while the lighter regions represent the graphite matrix. It is in this matrix, composed of smaller particles chemically and mechanically joined, which are arranged the graphite blades.

In order to verify the changes caused in the graphite structure, more specifically in the basal plane of the sample due to milling, Fig. 18 shows the images of the fractured (a) and

machined (b) surfaces of the graphite with a $\times 30,000$ magnification.

In the image of the fractured surface, it is possible to identify the graphite slides similar to those identified by Hutchings [33] and Paulchamy et al. [34], overlapping more symmetrically compared with the image of the machined surface. In this image, it is also possible to notice one of the properties of the graphite, the brittleness, due to the almost flat rupture of the blades of the material.

With respect to the machined surface, the figure shows that the region that passes through the cutting process, in addition to presenting graphite shear, also generates high deformations in the material and a high amount of blade breakage. According to Pierson [31], this phenomenon requires a high amount of energy due to the covalent bond of the carbon atoms of the graphite structure, what can be a possible cause for the abrasive power of the graphite.

This structure was noted regardless of the treatment applied in the tools. It was a result of the cutting process of the milling which affected the mechanisms and the types of wear present in the tools during the machining of the graphite, as can be visualized in the images of Fig. 15.

4 Conclusion

The results obtained through the execution of this work contributed to the better understanding on the cutting-edge treatments performed in milling cutters and their impacts during the machining of graphite electrodes.

The SEM analyzes indicated a surface with an apparent reduction in the width of the crystals, both for the tools that passed through the abrasive brushes polishing process and

those that went through the drag finishing process, and in the tools with FD an apparent rounding of the edges of the crystals was also visible.

The roughness measurements on the tools showed a gain in the finishing of the treated tools by 23%. The finishing processes tested presented statistically the same roughness values; however, the FD process presented a smaller variation, both in comparison with PAB process and with the OS treatment.

The graphite characterization showed the changes caused due to the machining process in the material structure, the most relevant being the deformations in the basal plane of the graphite, which may be a possible explanation for the high abrasive power of the material.

With the tool life graphic, it is possible to verify the smaller slope of the curves of the PAB and FD tools compared with the OS, which indicated the least wear during the tests. A similar behavior on these is also noticeable, but a remarkable difference is the smaller variation of the results with respect to the curve of the FD tool.

The OS tools presented the end of life with a machined average length of 1,126 m, PAB tools with 1,663 m, and FD tools with an average of 1,840 m, which present a gain of 47% and 63%, respectively.

Overall, all tested tools obtained the same wear mechanisms and types, being the abrasion the main wear mechanism, which caused the flank, crater, and notch wear. And the two cutting-edge treatments showed gains and demonstrated their potential to be applied in production tools.

Acknowledgments This study could not have been completed without the cooperation and technical support of UCS, CAPES and cooperation and availability of Sulbras Moldes e Plásticos.

References

- Klocke F, König W (2008) *Fertigungsverfahren 1: Drehen, Fräsen, Bohren*, 8th edn. Springer Verlag, Aachen, 504 p
- Cabral G, Reis P, Polini R, Titus E, Ali N, Davim JP, Grácio J (2006) Cutting performance of time-modulated chemical vapour deposited diamond coated tool inserts during machining graphite. *J Diamond Relat Mater* 15:1753–1758
- Astakhov VP, Shvets SV, Osman MOM (1997) Chip structure classification based on mechanics of its formation. *J Mater Process Technol* 71:247–257
- Lei X, Wang L, Shen B (2013) Comparison of chemical vapor deposition diamond-, diamond like carbon- and TiAlN-coated microdrills in graphite machining. *Proc Inst Mech Eng B J Eng Manuf* 227:1299–1309
- Wan Z et al (2015) Mechanism of material removal during orthogonal cutting of graphite/polymer composites. *Int J Adv Manuf Technol* 82(9-12):1815–1821
- Almeida FA, Sacramento J, Oliveira FJ, Silva RF (2008) Micro and nano-crystalline CVD diamond coated tools in the turning of EDM graphite. *J Surf Coat Technol* 203:271–276
- Schroeter RB, Kratochvil R, Gomes JO (2006) High-speed finishing milling of industrial graphite electrodes. *J Mater Process Technol* 179:128–132
- Heaney PJ, Sumant AV, Torres CD, Carpick RW, Pfefferkorn FE (2008) Diamond coatings for micro end mills: enabling the dry machining of aluminum at the micro-scale. *J Diamond Relat Mater* 17:223–233
- Harano K, Satoh T, Sumiya H (2012) Cutting performance of nanopolycrystalline diamond. *J Diamond Relat Mater* 24:78–82
- Zeilmann ZP, Vacaro T, Dos Reis ES, Westphal CJ (2013) Desempenho de fresas de aço-rápido após tratamento superficial. In: 7º Congresso brasileiro de engenharia de fabricação, Itaitiaia, Rio de Janeiro, Brasil
- Bhattacharyya P, Sengupta D, Mukhopadhyay S (2007) Cutting force-based real-time estimation of tool wear in face milling using a combination of signal processing techniques. *Mech Syst Signal Process* 21:2665–2683
- Ralchenko VG, Aahkinazi EE, Zavedeev EV, Khamich AA, Bolshakov AP, Ryzhkov SG, Sovik DN, Shershulin VA, Yurov VY, Rudnev VV (2016) High-rate ultrasonic polishing of polycrystalline diamond films. *J Diamond Relat Mater* 66:171–176
- Tsai HY, Ting CJ, Chou CP (2006) Evaluation research of polishing methods for large area diamond films produced by chemical vapor deposition. *J Diamond Relat Mater* 16:253–261
- Murakawa M, Takeuchi S, Alahelisten A, Kasugai M (1996) An efficient mechanical polishing method for diamond-coated inserts and testing of their performance. *J Surf Coat Technol*:686–691
- Bouzakis KD, Michailidis N, Skordaris G, Bouzakis E, Biermann D, M'saoubi R (2012) Cutting with coated tools: coating technologies, characterization methods and performance optimization. *CIRP Ann* 61:703–723
- Denkena B; Breidenstein B (2011) Cohesive damage of PVD-coated cutting tools – a result of the residual stress distribution. 9th Int. Conf. “The Coatings”, Thessaloniki, Greece, 3–5 October, p 89–97
- Rodríguez CJC (2009) Cutting edge preparation of precision cutting tools by applying micro-abrasive jet machining and brushing. 2009. 205 f. Doctorate Thesis, Kassel University, Germany
- Overholser RW, Stango RJ, Fournelle (2003) Morphology of metal surface generated by nylon/abrasive filament brush. *Int J Mach Tools Manuf* (43):193–202
- OTEC, Edge Rounding and polishing of tools. Presentation, 2008.
- Uhlmann E, Oberschmidt D, Kuche Y, Löwenstein A (2014) Cutting edge preparation of micro milling tools. *Procedia CIRP*: 349–354
- TOKAY Carbon. Graphite Electrode. <http://www.tokaicarbon.jp>. Access: 04 March 2018.
- Ost CA (2016) Análise da qualidade superficial no fresamento de aço P20 com diferentes tratamentos de ferramentas e condições de lubrificarrefrigerantes. (Portuguese). Dissertation (Master Mechanical Engineering). Posgraduate Programm. Universidade de Caxias do Sul, Caxias do Sul
- OTEC. Mídias para processo a seco. Disponível em: <http://www.otec.de/pt/produtos/media/processo-a-seco/casca-de-noz-granulada/>. Access: 04 April 2017.
- Tikal F (2009) Schneidkantenpräparation: Ziele. Kassel University Press, Verfahren und Messmethoden
- Gunnars J, Alahelisten A (1996) Thermal stresses in diamond coatings and their influence on coating wear and failure. *Surf Coat Technol* 80:303–312
- Machado AR, Coelho RT, Abrão AM, Silva MB (2009) Teoria da usinagem dos materiais, 9th edn. Blucher, 384 p, São Paulo
- Zeilmann RP, Fontanive F, Soares RM (2017) Wear mechanisms during dry and wet turning of Inconel 718 with ceramic tools. *Int J Adv Manuf Technol* 92:2705–2714

28. Li Q, Gong Y, Sun Y, Liu Y, Liang C (2018) Milling performance optimization of DD5 Ni-based single-crystal superalloy. *Int J Adv Manuf Technol* 94:2875–2894
29. Cabral G, Gäbler J, Lidner J, Grácio J, Polini R (2008) A study of diamond film deposition on WC-co inserts for graphite machining: effectiveness of SiC interlayers prepared by HFCVD. *J Diamond Relat Mater* 17:1008–1014
30. Zeilmann RP, Zanella C (2018) Tool wear coated with PCD in high-speed milling of graphite. *Int J Adv Manuf Technol* 97: 1497–1503
31. Pierson HO (1993) *Handbook of carbon, graphite, diamond and fullerenes: properties, processing and applications*. Noyes Publications, 417 p, New Jersey
32. Huo D, Lin C, Dalgarno K (2014) An experimental investigation on micro machining of fine-grained graphite. *Int J Adv Manuf Technol* 72(5-8):943–953
33. Hutchings IM (1992) *Tribology – Friction and wear of engineering materials*. Department of materials science and metallurgy. University of Cambridge, London. 278 p
34. Paulchamy B, Arthi G, Lignesh BD (2015) A simple approach to stepwise synthesis of graphene oxide nanomaterial. *J Nanomed Nanotechnol* 06

Publisher's note Springer Nature remains neutral with regard to jurisdictional claims in published maps and institutional affiliations.